

Theory and Practice of a Small Toner-Charge-Spectrometer

*Andreas Küttner, Reinhold H. Epping
Epping GmbH, D - 85375 Neufahrn, Germany
Reinhold Hess, Matthias G. Hackenberg*

*GMD German National Research Center for Information Technology
Institute for Algorithms and Scientific Computing (SCAI)
Schloss Birlinghoven, D-53754 Sankt Augustin, Germany*

Abstract

At the IS&T- NIP11 conference 95 in Hilton Head, South Carolina we made a short introduction of the concept of our new *q-test* machine. The device is a small low cost 'toner charge spectrometer', which is easy to handle with good reproducibility. Now this machine is available with a microscope scanning unit and analysis software. The inhomogeneous geometry of the electric field and the airflow in the measurement cell leads to some advantages in handling the measurement and to the results in the area of toner charge and diameter, but makes a complex calculation necessary. First results will show the reproducibility of the unit and make a direct comparison to other charge spectrometers (e.g. *q/d-meter*) possible.

The device is not only designed for the R&D department, even the quality control can have a quick and easy proof of the *q/d* distribution of the powder.

Introduction

The *q/d*-distribution is today one of the important parameters in the development and in the characterization of dry toner. Therefore different charge spectrometers with different measurement methods have been developed. Two are commercially available. Most of these machines use a laminar airflow and a homogenous electric field [1]. This makes the calculation of the *q/d* - distribution relatively easy, but the hardware is getting more complex and larger. In the *q-test* machine we have gone the opposite way. The machine is a small and easy to handle construction, with a complex geometry, that makes the evaluation more extensive. The *q-test* method was first introduced at the NIP 11 in Hilton Head, South Carolina [2]. The following is a short description.

Description

The *q-test* was developed from the *Epping q/d-meter*, but with the idea of an easy-to-handle unit for use in the R&D department as well as for the quality and the process control.

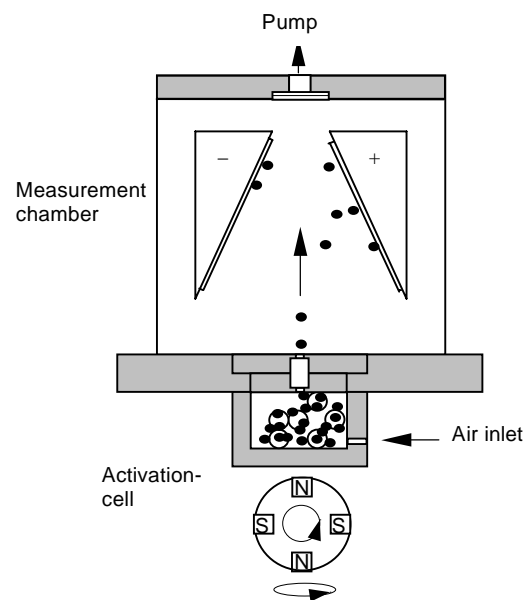


Figure 1. Cross section of the *q-test* with a two component activation cell

Construction

The *q-test* is divided into two separate desktop units – the measurement unit with the measurement chamber and the scanning unit with the microscope.

The measurement unit uses a air-stream with a crossed electrical field, as it is known from the *Epping q/d-meter*. A cross section of the measurement unit is shown in Figure 1. Instead of the laminar airflow a 'free air stream' is used and instead of the homogeneous electric field the pair of electrodes are angled, so that the electric field strength increases in direction of the air stream.

The scanning unit consists of a cross table and the microscope with the CCD-camera for the image analyzing system. The scanning and the evaluation is made automatically by the software. The toner deposition is scanned in x/y-direction.

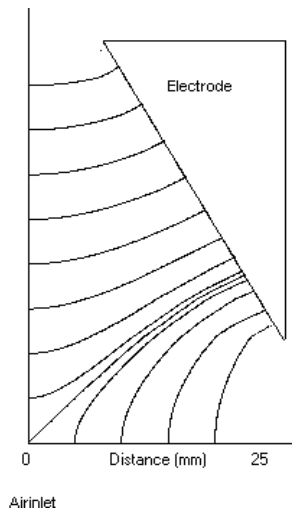


Figure 2. Electrical field lines in the measurement chamber

Measurement Method

The toner is sucked from the activation cell or other units (e.g. directly from the developer roll or the photoconductor) and is transported with the air stream through the electric field, where it is deflected onto the electrodes according to the charge to diameter ratio. Both polarities are determined by one measurement. On the electrodes a slice of glass is placed which can easily be removed. The two slices with the toner deposition are placed in the scanning unit and are evaluated. For a simple control of the charge distribution a visual comparison of the deposition is useful.

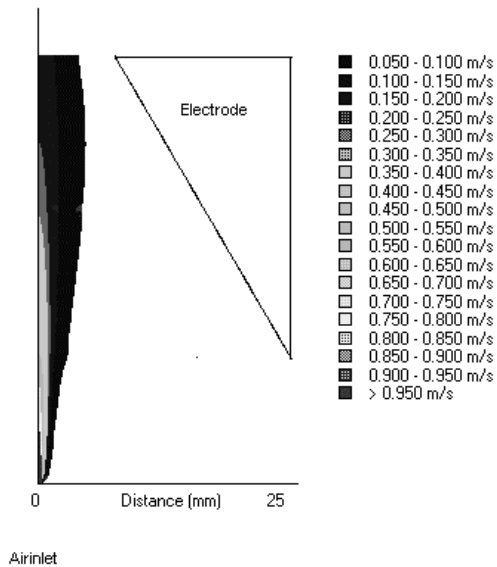


Figure 3. Air beam in measurement chamber

Activation Cells

One advantage of the *q*-test is that the measurement chamber is a small unit and can easily be adapted to the special demands of the application. The air stream in the chamber is sucking, so that no additional airflow is

necessary to pull the particles from surfaces into the chamber. There are different kinds of standard activation cells available for the different types of toner, e.g. two component systems, mono-component magnetic and mono-component nonmagnetic toners. These units are also used in the *q/d-meter*. The standard cells are prepared from original cartridges, so that almost the same conditions as in the target machine are found. A unit to suck off from the photoconductor is also available.

Calculation of the Toner Deposition

As was mentioned before the calculation of the toner path through the measurement chamber is more complex, because of the inhomogeneous geometry. The toner particle movement in the air stream is affected by the electrical field force, the frictional force and the gravitational force. This is described with a system of two dependent differential equations [3] for the axial (*y''*) and the radial acceleration (*x''*) of the toner particle.

$$y'' = E_y(x,y) \cdot q/m - F_r(y'(x,y))/m - g \tag{1}$$

$$x'' = E_x(x,y) \cdot q/m - F_r(x'(x,y))/m \tag{2}$$

with E_x and E_y the electric field strength in the *x* and *y* direction, respectively, the air resistance F_r , the gravitational acceleration *g* and the mass of the particle *m*. $E_y(x,y)$ and $E_x(x,y)$ is given through a matrix, which is calculated with the finite volume method on the GMD Institute (see chapter 'Numerical Simulation'). Figure 2 shows the electric field lines in the measurement chamber, The velocity of the particle *y'* and *x'* depends strongly on the air-velocity $v_{air,y}(x,y)$ and $v_{air,x}(x,y)$ (see figure 3), which is also given through a matrix, prepared by GMD with the same method. Because of the symmetry only one half of the measurement chamber is shown in Figure 2 and 3. The differential equations were solved with a numerical approximation method. The calculation of the gravitational force can be adjusted by the software depending on the mounting position of the measurement chamber.

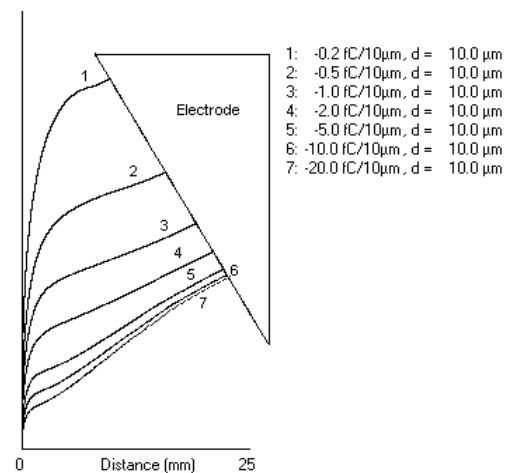


Figure 4. Calculated track of toner particles with different charges

Figure 4 shows the calculated track and the deposition point of toner particles with the same size and different q/d values. The higher charged particles will be found very close together, while the low charged particles deposit in a broader area. The deposition point depends on the q/d value of the particle, so that the charge to diameter ratio of a toner is a function of its deposition point x on the glass slice - $q/d = f(x)$. This is shown in figure 5, where particles with the same q/d value but with different sizes have the same deposition point. By scanning the toner layer on the glass slices the q/d distribution can be calculated.

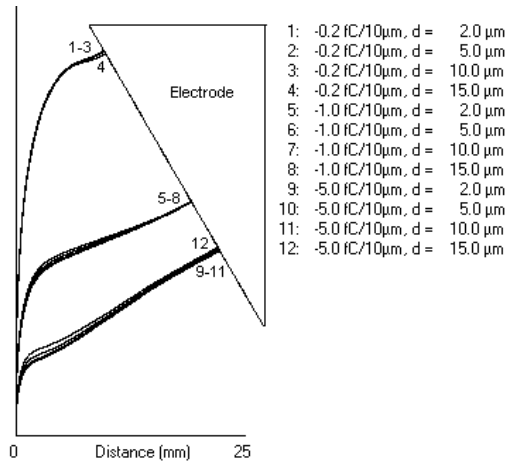


Figure 5. Calculated toner track in the measurement chamber, with constant q/d and variation of the diameter.

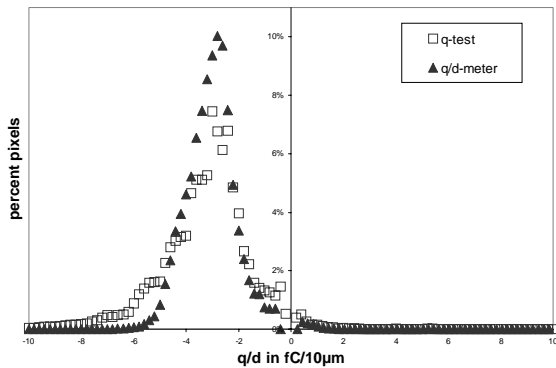


Figure 6. Comparison of the measured q/d -distribution of the q -test and the q/d -meter

Measurements

To prove the theoretical calculation, a comparison with the *Epping q/d-meter* has been made. The measurements were carried out under the same conditions and the same activation unit were used in both machines. It is seen from figure 6, that there is a good correlation between both machines. In the area of higher q/d -values ($>5fC/10µm$) the q -test shows higher values, because of the lower resolution in that area. Further, a series of 10 measurements were made to prove the reproducibility of the results (see figure

7). The mean q/d values of the measurements are shown in the figure.

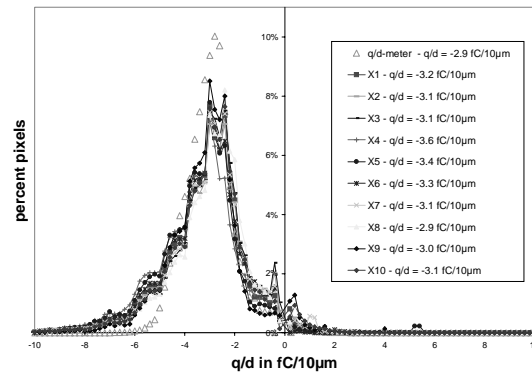


Figure 7. 10 measurements with the q -test under the same condition

Numerical Simulation

General Approach

The electrical field and the flow field of the air in the measurement chamber are numerically calculated with L_1SS [6], an environment for the parallel multigrid solution of partial differential equations on general domains. Highly efficient multigrid methods [4,7] are used in L_1SS . Block-structured grids consisting of logically rectangular blocks are combined with a finite-volume discretization. Parallelization is done by grid partitioning, i.e. the blocks are mapped to different processors of the parallel computer. As communication within the underlying communication library (CLIC) is performed by MPI, portability is guaranteed.

Electrical Field

For the electrical field in the central plane of the measurement chamber the Poisson equation

$$\Delta u = 0 \tag{3}$$

in two dimensions for the potential u is solved. Due to symmetry the two-dimensional calculation is a sufficiently good approximation for the potential in the three-dimensional domain.

Flow Field

The flow field is calculated using the steady incompressible Navier-Stokes equations in Reynolds number divided form

$$\begin{aligned} (u^2)_x + (uv)_y + (uw)_z + p_x &= 1/Re \cdot \Delta u \\ (uv)_x + (v^2)_y + (vw)_z + p_y &= 1/Re \cdot \Delta v \\ (uw)_x + (vw)_y + (w^2)_z + p_z &= 1/Re \cdot \Delta w \\ c^2 \cdot (u_x + v_y + w_z) &= 0 \end{aligned} \tag{4}$$

with velocities u, v, w , pressure p , a constant reference velocity c and Reynolds number Re . The three-dimensional

finite volume discretization described in [5] is used within L_sSS . Moreover, complex boundary conditions, such as pressure extrapolation at internal corners, or symmetry conditions, have to be handled.

Due to the complex geometry of the measurement chamber the three-dimensional computation of the flow field is necessary. The results obtained by a two-dimensional computation of a cross section show an unexpectedly slowly decreasing velocity in inflow direction and a fast back stream flow at the sides of the computational domain. Because of symmetry the three dimensional computation has to be performed only for one quarter of the chamber. The computational domain and the coarse grid can be found in Figure 8.

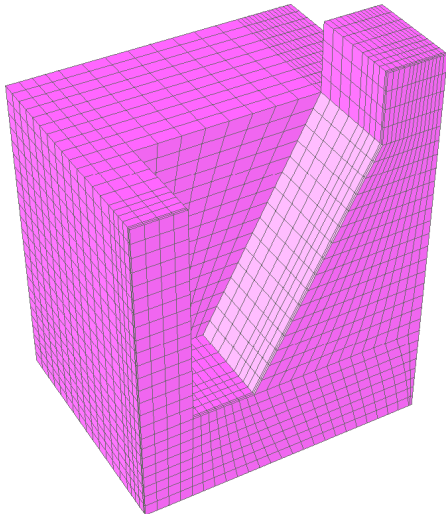


Figure 8. Domain and coarse grid for the three-dimensional computation

Hitherto, due to limitations of the grid generator, generation of three-dimensional grids for curved domains is not possible in each case. As a result of this, the round boundaries of the measurement chamber, the inlet and the outlet are approximated by rectangles. In spite of this simplification, the (quite complex) computational grid gives a good approximation to the actual chamber. A hierarchy of three grids is used within the multigrid cycles. The finest computational grid consists of 806,224 grid points in eight blocks. The coarsest grid, shown in Figure 8, is formed by 15,334 grid points. As four variables are located in each point of the computational grid, 3,717,320 unknowns have to be solved. The three-dimensional computation leads to distributed back stream flow and reduced velocity. Calculation is performed on nine nodes of a parallel high performance machine IBM SP2 for several hours. Unequal distribution of work caused by different sizes of blocks is the main draw-back with regard to computing time. The importance of this load-imbalance is likely to decrease with a new three-dimensional version of L_sSS , currently being

developed. Local refinements will lead to less grid points. In addition to a decrease in computing time, refinements will result in more accurate computations.

Acknowledgments

The development of the three-dimensional version of L_sSS is supported within the GRISLi project by the German Federal Ministry for Research and Education under contract no. 01IS512C.

Summary

The results show a good correlation with the *Epping q/d-meter* and good reproducibility. The *q-test* machine is a small, portable charge spectrometer for dry toner, which is easy to handle. The relatively small dimensions of the measurement chamber make it possible to mount it on the application (e.g. photoconductor, developer drum) and the toner sample can be taken directly from the target system. The toner deposition is fixed on glass slices and can be used for other investigations or can be stored as proof of quality of the toner in the production process.

References

1. L. B. Schein, *Electrophotography and Development Physics*, 2nd edition, Laplacian Press, p.87ff, (1996)
2. R. H. Epping and K. H. Schubeck, IS&T 11th International Congress on Advances in Non-Impact Printing Technologies, p.166ff, (1995)
3. M. Mehlin and R. M. Hess, *Journal of Imaging Science and Technology*, vol.36, no. 6, p. 142-150, (1992)
4. W. Joppich, S. Mijalkovic, *Multigrid Methods for Process Simulation*, Computational Microelectronics. Springer Verlag, Wien, New York, (1993)
5. C. W. Oosterlee, H. Ritzdorf, Flux difference splitting for three-dimensional steady incompressible Navier-Stokes equations in curvilinear co-ordinates, *International Journal for Numerical Methods in Fluids* 23, p.347–366(1996)
6. H. Ritzdorf, A. Schüller, B. Steckel, K. Stüben, L_sSS - An environment for the parallel multigrid solution of partial differential equations on general 2D domains, *Parallel Computing* 20, p.1559 – 1570 (1994)
7. K. Stüben, U. Trottenberg, *Multigrid Methods: Fundamental Algorithms*, *Model Problem Analysis and Applications*, *Lecture Notes in Mathematics* 960 p.1-176 (1982)

Biography

Andreas Küttner received his Engineering degree from Fachhochschule Munich in technical physics. He is working in the fields of computer programming and electrostatics. He has been a member of Epping GmbH since 1995 and serves as the Technical Director since 1997.